Human Molecular Genetics, 2012, Vol. 21, No. 5 **963–977**
doi:10.1093/hmg/ddr502
Advance Access published on November 1, 2011

The homocysteine-inducible endoplasmic reticulum (ER) stress protein Herp counteracts mutant α-synuclein-induced ER stress via the homeostatic regulation of ER-resident calcium release channel proteins

Cherine Belal[1], Neema J. Ameli[1], Adam El Kommos[1], Spencer Bezalel[1], Aziz M. Al'Khafaji[1], Mohamed R. Mughal[2], Mark P. Mattson[2], George A. Kyriazis[3], Björn Tyrberg[3] and Sic L. Chan[1,*]

[1]The Burnett School of Biomedical Sciences, College of Medicine, University of Central Florida, Orlando, FL, USA, [2]Laboratory of Neurosciences, National Institute on Aging Intramural Research Program, Baltimore, MD, USA and [3]Diabetes and Obesity Research Center, Sanford-Burnham Medical Research Institute, Orlando, FL, USA

Received July 6, 2011; Revised October 5, 2011; Accepted October 28, 2011

Endoplasmic reticulum (ER) stress has been implicated as an initiator or contributing factor in neurodegenerative diseases. The mechanisms that lead to ER stress and whereby ER stress contributes to the degenerative cascades remain unclear but their understanding is critical to devising effective therapies. Here we show that knockdown of Herp (Homocysteine-inducible ER stress protein), an ER stress-inducible protein with an ubiquitin-like (UBL) domain, aggravates ER stress-mediated cell death induced by mutant α-synuclein (αSyn) that causes an inherited form of Parkinson's disease (PD). Functionally, Herp plays a role in maintaining ER homeostasis by facilitating proteasome-mediated degradation of ER-resident Ca^{2+} release channels. Deletion of the UBL domain or pharmacological inhibition of proteasomes abolishes the Herp-mediated stabilization of ER Ca^{2+} homeostasis. Furthermore, knockdown or pharmacological inhibition of ER Ca^{2+} release channels ameliorates ER stress, suggesting that impaired homeostatic regulation of Ca^{2+} channels promotes a protracted ER stress with the consequent activation of ER stress-associated apoptotic pathways. Interestingly, sustained upregulation of ER stress markers and aberrant accumulation of ER Ca^{2+} release channels were detected in transgenic mutant A53T-αSyn mice. Collectively, these data establish a causative link between impaired ER Ca^{2+} homeostasis and chronic ER stress in the degenerative cascades induced by mutant αSyn and suggest that Herp is essential for the resolution of ER stress through maintenance of ER Ca^{2+} homeostasis. Our findings suggest a therapeutic potential in PD for agents that increase Herp levels or its ER Ca^{2+}-stabilizing action.

INTRODUCTION

Parkinson's disease (PD) is a progressive neurodegenerative movement disorder that results from the degeneration of dopaminergic (DA) neurons in the substantia nigra (1). A common pathological feature of PD is the aggregation of α-synuclein (αSyn) into cytoplasmic inclusions called Lewy bodies in the degenerating DA neurons (1). Cell culture studies have shown that overexpression, impaired turnover and mutations lead to αSyn aggregation (2). Two missense mutations (Ala53Thr and Ala30Pro) in αSyn that cause early-onset, autosomal dominant forms of PD enhance the aggregation and toxicity of the protein (2). Duplication or triplication of the *αSyn* gene was also found to cause early-onset PD, suggesting that elevated levels of wild-type αSyn can also lead to neurotoxicity (3). It is not yet clear how αSyn aggregation induces the degenerative cascades leading to PD.

*To whom correspondence should be addressed at: 4000 Central Florida Blvd, Orlando, FL 32816. Tel: +1 4078233585; Fax: +1 4078230956; Email: schan@mail.ucf.edu

Recent studies have demonstrated that mutant αSyn may exert its pathological effects in parts by inactivating the Grp78/Bip chaperone function (4) or impeding endoplasmic reticulum (ER) to Golgi vesicular transport (5) leading to abnormal accumulation of proteins within the ER and induction of ER stress. Cells respond to ER stress by activating the unfolded protein response (UPR) aimed at inducing translational repression and expression of ER-resident chaperones to enhance protein folding, processing and degradation of misfolded proteins, thus relieving cells from ER stress (6). Prolonged or unmitigated ER stress associated with insufficient degradation of misfolded proteins or deranged Ca^{2+} homeostasis would subsequently activate ER stress-associated apoptotic pathways (7).

Hallmarks of ER stress are detected in several experimental models of PD (8,9) and in nigral DA neurons of PD subjects (10). Expression of PD-linked mutant αSyn elevates CCAAT/enhancer-binding protein homologous protein (CHOP) (11), an ER stress-induced apoptotic mediator (12). CHOP is also elevated in neurotoxin models of PD (8,9) and is a critical mediator of apoptotic death in substantia nigra dopamine neurons (13). Salubrinal, a neuroprotective agent that acts to inhibit ER stress, protects cells from death induced by overexpression of mutant αSyn (11). Furthermore, ER stress is closely associated with the aggregation of αSyn in DA neurons (10). Although these studies suggest that ER stress is of pathophysiological relevance in PD, the underlying mechanisms of ER stress-mediated degenerative cascades and the specific roles of the various UPR proteins in PD pathogenesis remain unknown.

Herp (Homocysteine-inducible ER stress protein) is an ER integral membrane protein with the N-terminal ubiquitin-like (UBL) domain projecting into the cytosol (14). Upregulation of Herp is essential for neuronal survival as Herp knockdown enhances vulnerability to ER stress-induced apoptosis (15,16). How Herp contributes to the restoration of ER homeostasis remains unclear. Herp appears to stabilize ER Ca^{2+} homeostasis and mitochondrial function in neural cells subjected to ER stress (16). Herp may also play an essential role in ER-associated protein degradation (ERAD), the primary mechanism of misfolded protein degradation, as its knockdown results in the selective accumulation of ERAD substrates (17).

Recent studies demonstrated that Herp is induced in PD substantia nigra and is present in the core of Lewy bodies (18). The roles of Herp in PD remain unknown. Because Herp was shown to be critical for survival adaptation in the neurotoxin models of PD (19), we investigated whether Herp may counteract the neurodegenerative cascades caused by induced expression of mutant αSyn. We found that Herp plays an essential role in suppressing mutant αSyn-induced activation of ER stress-associated apoptosis signaling by inhibiting the deregulated ER Ca^{2+} release associated with the aberrant accumulation of ER resident Ca^{2+} release channels.

RESULTS

Expression of mutant αSyn evokes a sustained ER stress response

Previous studies provide evidence that mutant αSyn triggers a cell death program that involves activation of the ER stress response (11). It is yet not clear which and how ER stress proteins contribute to mutant αSyn-induced cell death. To investigate the role of Herp in the mutant αSyn-induced degenerative process, we generated tetracycline (Tet)-inducible pheochromocytoma 12 (PC12) cells. Time course analysis indicated that the αSyn protein level reaches a plateau 48 h after induction (Fig. 1A). Concurrently, mRNA and protein levels of the ER stress markers Grp78 and Herp were markedly elevated in the PC12 cells expressing mutant αSyn, especially those expressing A53TαSyn (PC12-A53TαSyn), when compared with PC12 cells expressing wild-type αSyn (PC12-WTαSyn) (Fig. 1B). Levels of CHOP were also markedly higher in PC12-A53TαSyn (Fig. 1B), suggesting that at this expression level, there was a selective deleterious effect of A53TαSyn but not WTαSyn. Similar results were obtained in PC12 cells transiently expressing A53TαSyn and WTαSyn (Fig. 1C).

Herp protects against mutant αSyn-induced cell death

Compared with PC12 cells stably expressing the empty vector (PC12-VT), PC12-WTαSyn and PC12-A30PαSyn, PC12-A53TαSyn exhibits significantly higher baseline cell death (Fig. 2A) which correlated with increased CHOP protein level and caspase-12 (Casp12) activation (Fig. 2B). Because A53TαSyn enhances activation of ER stress-related apoptosis signaling, we utilized PC12-A53TαSyn in subsequent knockdown studies. PC12-A53TαSyn treated with a small interference RNA (siRNA) targeting Herp (siRNA-Herp) but not a non-silencing control siRNA (siRNA-Con) exhibited higher basal rate of cell death (Fig. 2C). In contrast, ectopic expression of Herp, but not the dominant-negative mutant Herp that lacks the UBL domain (ΔUBL-Herp; Fig. 2D), significantly improved the viability of PC12-A53TαSyn (Fig. 2E). Notably, ΔUBL-Herp appeared to potentiate A53TαSyn-induced cell death consistent with a dominant-negative action of ΔUBL-Herp as reported previously (19).

Mutant αSyn perturbs ER Ca^{2+} homeostasis during ER stress

Given that Herp protects from A53TαSyn-induced death (Fig. 2C and E) and that Herp plays a crucial role in stabilizing ER Ca^{2+} homeostasis in ER-stressed PC12 cells (16), we next determined whether A53T-αSyn may perturb ER Ca^{2+} regulation by altering the activity of the two main classes of ER-resident Ca^{2+} release channels, IP_3R (inositol triphosphate receptor) and RYR (ryanodine receptor) which can be activated by their respective agonists, bradykinin (BK) and caffeine (20–22). The average peak amplitude of BK-evoked Ca^{2+} release in the absence of extracellular Ca^{2+} was significantly larger in PC12-A53TαSyn when compared with PC12-WTαSyn and PC12-VT (Fig. 3A), indicating that A53TαSyn enhances ER Ca^{2+} release. No significant difference was observed in thapsigargin-induced depletion of ER Ca^{2+} store (Supplementary Material, Fig. S1A), suggesting that the ER stress-induced perturbation of the intracellular Ca^{2+} level ($[Ca^{2+}]i$) in PC12-A53TαSyn cannot be explained

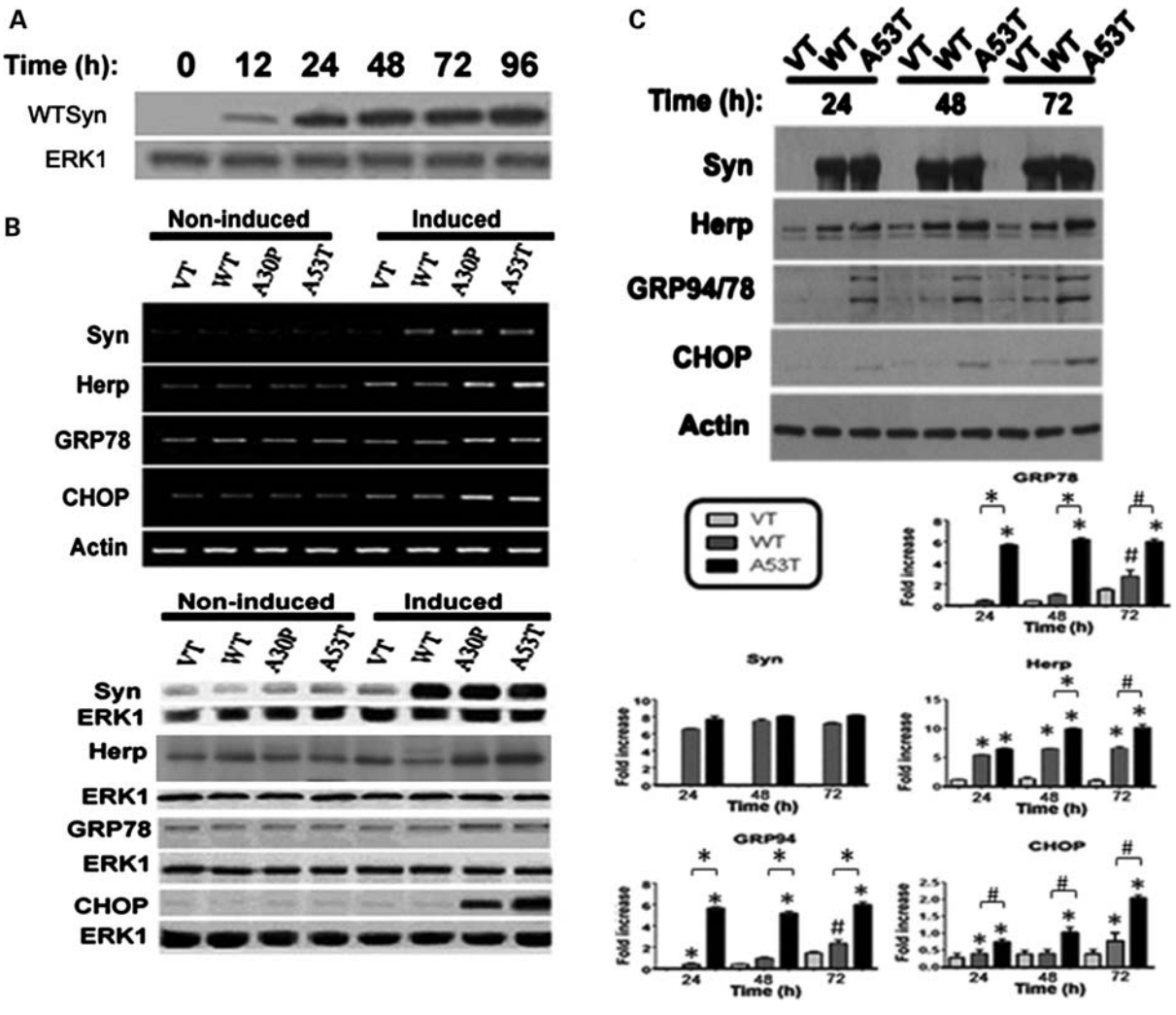

Figure 1. Expression of mutant αSyn induces a heightened ER stress response. (**A**) A representative immunoblot showing the time course of wild-type (WT) human αSyn protein level after the addition of Tet. The antibody used was specific for human αSyn. (**B**) Representative gel images (top) and immunoblots (bottom) of WT and mutant (A30P and A53T) αSyn, Herp, Grp94/78 and CHOP mRNA and protein levels, respectively, in PC12 cells 72 h after the addition of Tet (induced) or vehicle (non-induced). PCR products amplified were separated on ethidium bromide-stained agarose gels. Blots were reprobed with ERK1 to confirm equality of total protein loading. (**C**) Representative immunoblots (top) and results of densitometric analysis (bottom) of Herp, Grp94/78 and CHOP protein levels in PC12 cells at the indicated time points following transient transfection with either WT or mutant (A53T) αSyn. Control cells were transfected with the empty vector (VT). The antibody used was specific for human αSyn. Values are the mean ± SEM of three independent experiments. $^{\#}P < 0.05$; $^{*}P < 0.01$, compared with PC12-VT and PC12-WTα-Syn and between the indicated groups.

by higher ER luminal Ca^{2+} but rather is caused by a higher fraction of ER Ca^{2+} being released via IP_3R.

Tunicamycin (Tuni) is a classical ER stressor that induces a sustained increase in ER stress proteins (Supplementary Material, Fig. S1B). The magnitude of the BK-evoked Ca^{2+} release was also higher in PC12 cells treated with Tuni (PC12-Tuni) when compared with control cells that were left untreated or treated with vehicle (data not shown; 16,19). Consequently, treatment with BAPTA-AM, a cell permeable Ca^{2+} chelator, markedly improves the viability of both PC12-A53TαSyn and PC12-Tuni (Fig. 3B), suggesting that Tuni and A53TαSyn increase susceptibility to ER stress-induced death by enhancing ER Ca^{2+} release.

Mutant αSyn-induced ER stress perturbs homeostatic regulation of ER-resident Ca^{2+} release channels

Next, we determined whether the heightened cytosolic Ca^{2+} level in PC12-Tuni and PC12-A53TαSyn results from altered homeostatic regulation of ER-resident Ca^{2+} release channels. Three distinct types of IP_3Rs (types 1–3) have been cloned in mammals and each type shows distinct properties in terms of their IP_3 sensitivity, modulation by cytoplasmic Ca^{2+} concentration and unique tissue distribution (23,24). Among them, the type 1 IP_3R (IP_3R1) is highly expressed in the central nervous system (24). Quantitative real-time PCR (qRT-PCR) analysis showed that IP_3R1 is the

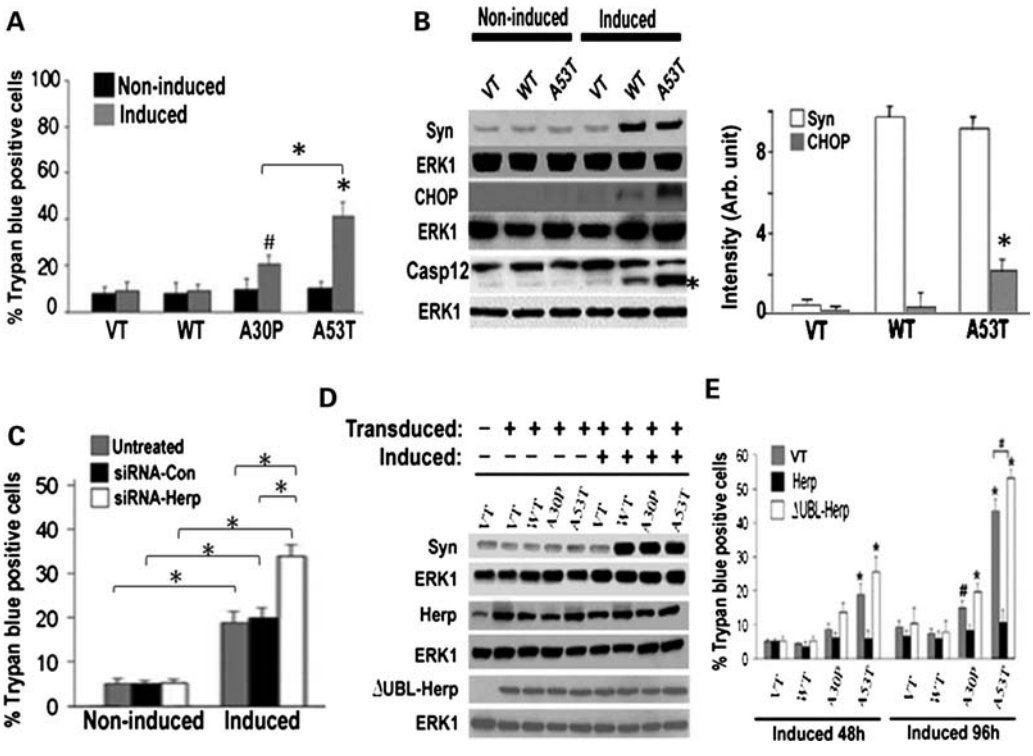

Figure 2. Herp protects from mutant αSyn-induced cell death. (**A**) Trypan blue exclusion was used to determine the viability of the indicated PC12 clones at 96 h under induced or non-induced conditions. Data represent the mean ± SEM of three separate experiments. $^{\#}P < 0.05$,$^{*}P < 0.01$, compared with PC12-WTαSyn and PC12-VT under non-induced and induced conditions; $^{*}P < 0.01$, between the indicated clones expressing mutant αSyn. (**B**) Representative immunoblots of protein levels of αSyn and CHOP and Casp12 processing in the indicated PC12 cells 72 h after the addition of Tet (induced) or vehicle (non-induced). Appearance of the active proteolytic fragment of Casp12 is indicated by an asterisk. ERK is used as an internal control of protein loading. Histogram shows densitometric analysis of CHOP protein. $^{\#}P < 0.05$, versus the PC12-WTαSyn and PC12-VT under non-induced and induced conditions; (**C**) histograms show the viability of the PC12-A53T after transfection with siRNA-Con and siRNA-Herp (100 nM). One day after transfection, Tet was added to the cultures and cell viability was determined 48 h after by trypan blue exclusion. Values represent the mean ± SEM of three separate experiments. $^{\#}P < 0.05$, $^{*}P < 0.01$ compared with respective non-induced and between the indicated induced PC12 cells. (**D**) Representative immunoblots of αSyn, Herp and ΔUBL-Herp protein levels in the indicated PC12 cells under non-induced (−) or induced (+) conditions for 48 h. PC12 cells were transduced with viral particles expressing empty vector or vector containing Herp or ΔUBL-Herp construct 48 h prior to induction. ERK is used as an internal control of protein loading. (**E**) Histograms show the viability of the indicated PC12 cells after ectopic expression of Herp and ΔUBL-Herp. Trypan blue exclusion was used to determine cell viability 48 and 96 h after induction. Values represent the mean ± SEM of three separate experiments. $^{\#}P < 0.05$, $^{*}P < 0.01$, compared with groups transduced with the empty vector or Herp and between the indicated transduced groups.

major form of the receptor expressed in PC12 cells (Supplementary Material, Fig. S1C). PC12 cells also express detectable RYR1 and RYR3 (pan-RyR) (20,21). PC12-Tuni exhibit marked accumulation of IP_3R1 and pan-RyR protein (Fig. 3D; Supplementary Material, Fig. S1D) consistent with the notion that Tuni-induced ER stress leads to disruption of ER Ca^{2+} homeostasis (16). Expression of A53TαSyn also induces a marked increase in the protein levels of IP_3R1 (Fig. 3E) and pan-RyR (Fig. 3F), suggesting that the aberrant accumulation of ER Ca^{2+} release channels was likely mediated through an ER stress-related mechanism. Consistent with the elevated pan-RYR protein levels, PC12-Tuni and PC12-A53TαSyn were more vulnerable to cell death in the presence of caffeine when compared with their respective controls (Supplementary Material, Fig. S1E). In contrast, level of presenilin1 (PS1), which functions as a passive ER Ca^{2+} leak channel (25), was not markedly altered by ER stress (Fig. 3D and E). It is worth noting that unlike the increase in ER stress proteins which are mediated by a transcriptional mechanism (6,7), the ER stress-associated accumulation of IP_3R1 and pan-RYR was independent of transcription (Supplementary Material, Fig. S1F and G).

Inhibition of deregulated ER Ca^{2+} release ameliorates ER stress-mediated cell death and αSyn aggregation

Because ER-released cytosolic Ca^{2+} plays a critical role in the activation of several death effector pathways (16), we next determined whether blockade of ER Ca^{2+} release may ameliorate ER stress-induced cell death. Xestospongin C (a blocker of IP_3R) and dantrolene (a RyR blocker) at doses that did not cause robust death within 24 h substantially improved the viability of PC12-Tuni (Fig. 4A) and PC12-A53TαSyn (Fig. 4B). Neither IP_3R nor RyR inhibition altered the expression of αSyn (data not shown), thereby confirming that inhibition of the ER Ca^{2+} release rather than reduced expression of A53T-αSyn contributes to cell protection.

To further determine whether these ER-resident Ca^{2+} release channels are responsible for the heightened sensitivity of PC12-A53TαSyn to ER stress-mediated cell death, we

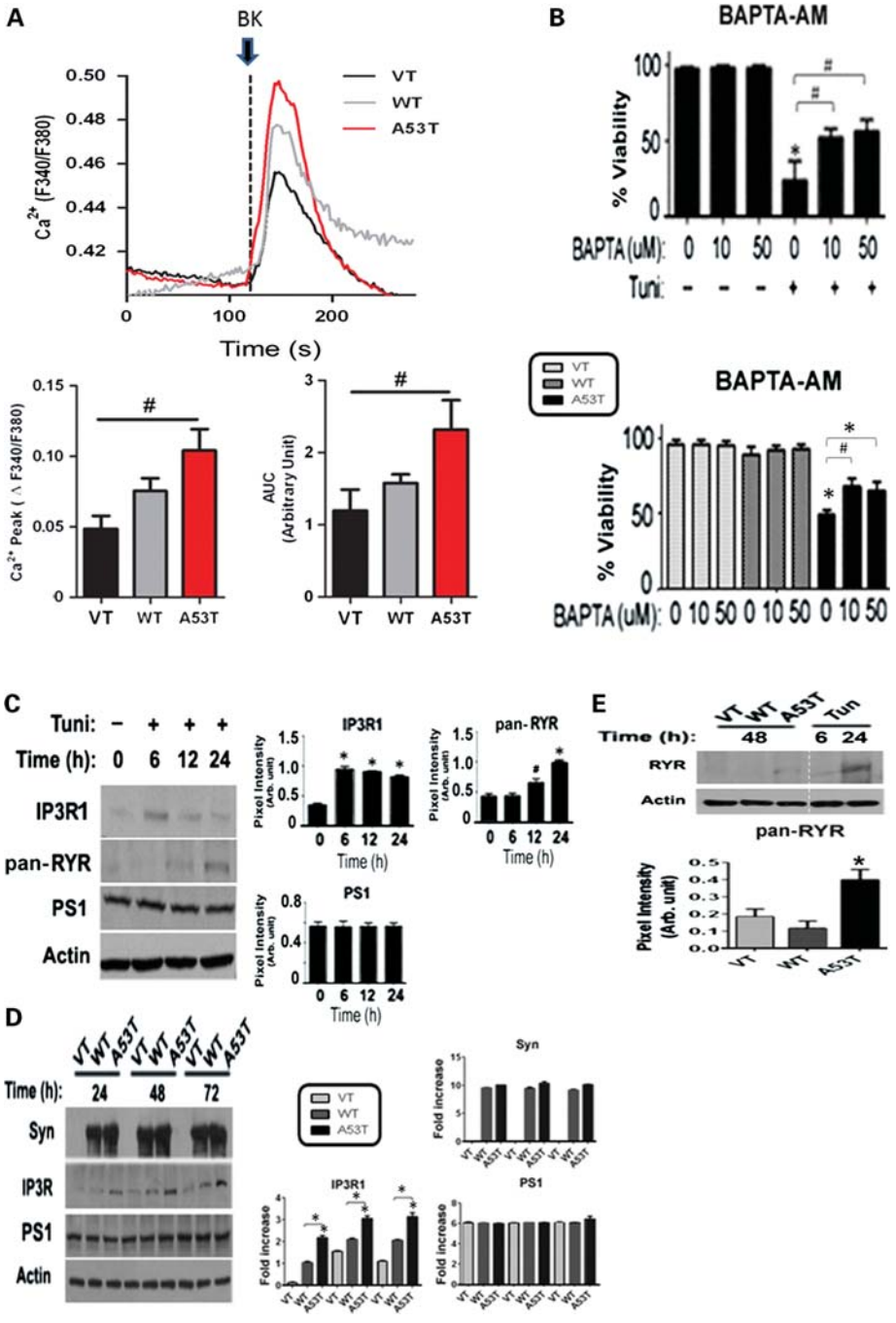

Figure 3. ER stress-induced by Tuni and mutant α-Syn perturbs ER Ca^{2+} homeostasis through the aberrant accumulation of ER-resident Ca^{2+} release channels. (**A**) Representative recordings of the BK (10 μM) -induced elevation of intracellular Ca^{2+} ($[Ca^{2+}]i$) in PC12 cells 48 h after expression of wild-type (WT) and mutant (A53T) αSyn. PC12 cells transfected with empty vector (VT) were included as controls. Cells were loaded with fura-2 and $[Ca^{2+}]_i$ was recorded in Ca^{2+} free medium as described under 'Materials and Methods'. Arrow indicates time of BK addition. Histograms show Ca^{2+} peak values (change from baseline) and AUC. Values are the mean ± SEM of determinations made in four to six separate cultures (15–20 cells assessed/culture). $^{\#}P < 0.05$, compared with VT. (**B**) Histograms show the percent of viable cells after treatment of PC12-Tuni (top) and PC12-A53TαSyn (bottom) with the indicated doses of BAPTA-AM. PC12 cells were pretreated with BAPTA-AM 2 h prior to either exposure to Tuni (20 μg/mL) or expression of VT, WT and A53T. Cell viability was determined 24 h after by Trypan blue exclusion. Values represent the mean ± SEM of three separate experiments. $^{*}P < 0.01$, $^{\#}P < 0.05$, compared with vehicle or VT at each time point and between the indicated groups. (**C**) Representative immunoblots (left) and results of densitometric analyses (right) of IP3R1, pan-RYR and PS1 protein levels in PC12-Tuni at the indicated time points. Values represent the mean ± SEM of three independent experiments. $^{*}P < 0.01$, $^{\#}P < 0.05$ compared with the untreated group. (**D**) Representative immunoblots (left) and results of densitometric analyses (right) of α-Syn, IP3R1 and PS1 protein levels in PC12 cells at the indicated time points after expression of VT, WT or A53T. Values represent the mean ± SEM of three separate experiments. $^{\#}P < 0.05$, $^{*}P < 0.01$, compared with VT and WTαSyn. (**E**) A representative immunoblot (top) and results of densitometric analysis (bottom) of the pan-RYR protein in PC12 cells at the indicated time points after expression of VT, WT or A53T. The Tuni-treated samples were included as positive controls for ER stress-induced increase in pan-RyR protein level. $^{*}P < 0.01$, compared with VT and WT. Equal protein loading in the immunoblots shown in (*C*)–(*E*) was confirmed after reprobing the membranes for actin.

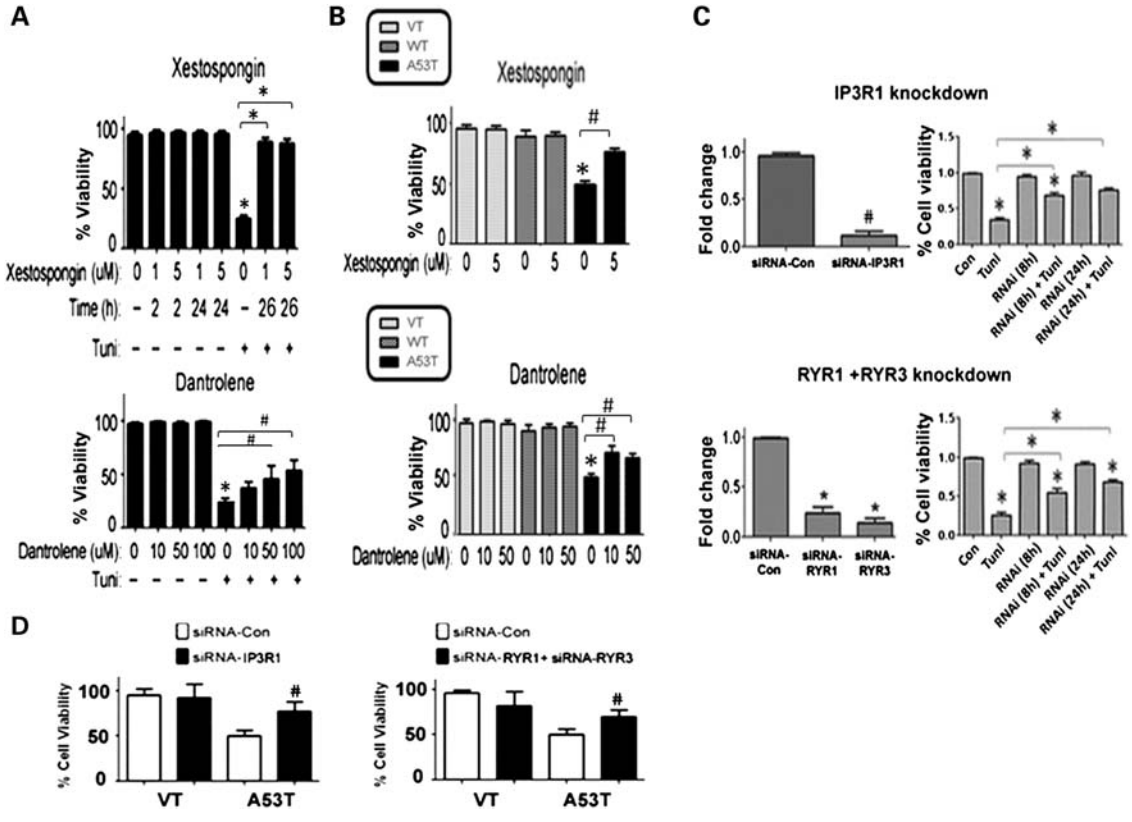

Figure 4. Pharmacological inhibition or gene knockdown of ER-resident Ca^{2+} release channels ameliorates ER stress-induced cell death. (**A**) Histograms show the percent of viable PC12 cells after treatment with Tuni (20 μg/ml) (+) or vehicle (−) for 24 h in the absence or presence of the indicated doses of xestospongin C (an IP3R blocker) or dantrolene (a RyR blocker). Both drugs were added 2 h prior to Tuni. Values are the mean ± SEM of three independent experiments. $^{\#}P < 0.05$; $^{*}P < 0.01$, compared with vehicle control and between the indicated groups. (**B**) Histograms show the percent of viable PC12 cells expressing empty vector (VT), wild-type (WT) and mutant (A53T) α-Syn. Xestospongin C (5 μM) or dantrolene (50 μM) were added 24 h after induction. Values are the mean ± SEM of three independent experiments. $^{\#}P < 0.05$; $^{*}P < 0.01$, compared with VT and WTα-Syn and between the indicated groups. (**C**) Histograms show the fold change of the indicated ER Ca^{2+} release channel, IP3R1 (top) or RYR1/RYR3 (bottom), in PC12 cells 24 h after transfection with the respective siRNAs (left panels) and the percent of viable transfected PC12 cells at the indicated time points after exposure to Tuni or vehicle (Con) (right panels). The siRNAs were added either 8 or 24 h (denoted by asterisk) prior to Tuni exposure. Values represent the mean ± SEM of three independent experiments. $^{\#}P < 0.05$; $^{*}P < 0.01$, compared with Con and between the indicated groups. (**D**) Histograms show the viability of the indicated PC12 cells in the presence of siRNA-IP3R1 (top) or siRNA-RYR1 and siRNA-RYR3 combined (bottom). Values represent the mean ± SEM of three independent experiments. $^{\#}P < 0.05$; $^{*}P < 0.01$, compared with siRNA-Con.

knocked down each channel protein at a time by using either siRNA-IP_3R1 or siRNA-RYR1 and siRNA-RYR3 in combination (Fig. 4C). The non-silencing control siRNA (siRNA-Con) alone did not alter IP3R1 nor RYR1/RYR3 expression (data not shown). A close correlation between protein levels of these ER Ca^{2+} release channels and the ER stress-induced apoptotic mediator CHOP was observed in PC12-Tuni (Fig. 4D) and PC12-A53TαSyn (Fig. 4E). CHOP which is known to be upregulated following a severe or prolonged ER stress was markedly suppressed along with Herp and Grp94/78 in PC12-Tuni transfected with the silencing siRNAs (Supplementary Material, Fig. S2A and B). These data suggest that impaired homeostatic regulation of ER-resident Ca^{2+} release channels might underlie chronic activation of ER stress and associated apoptosis signaling.

Because ER-released cytosolic Ca^{2+} plays a role in promoting αSyn aggregation (26), we next examined αSyn inclusion formation in PC12 cells transiently transfected with either WTαSyn or A53TαSyn tagged to enhanced green fluorescent protein (EGFP) by fluorescence microscopy. Xestospongin C substantially reduces not only the fraction of cells bearing cytoplasmic αSyn inclusions but also the size of the inclusions (Supplementary Material, Fig. S3). These fluorescent aggregates were not detected in PC12 cells transfected with EGFP alone (data not shown).

Herp counteracts ER stress through the homeostatic regulation of ER-resident Ca^{2+} release channels

Because Herp counteracts Tuni-induced cell death through the stabilization of ER Ca^{2+} homeostasis (16), we next determined whether Herp protects PC12-A53TαSyn (Fig. 2C and D) by a similar mechanism. Knockdown of Herp substantially increases the amplitude of the BK-induced Ca^{2+} transients (Fig. 5A) that result from the marked accumulation of IP_3R1 (Fig. 5B; Supplementary Material, Fig. S4A). Levels of pan-RYR but not PS1 proteins were also affected by Herp knockdown (Fig. 6B; Supplementary Material, Fig. S4A). Consequently, the deficits in Herp-dependent homeostatic regulation of ER Ca^{2+} release channels are also accompanied

by increased levels of the ER stress markers Grp94/78 and CHOP (Fig. 5B; Supplementary Material, Fig. S4A) and enhanced vulnerability to αSyn-induced death (Fig. 5C). Conversely, ectopic expression of Herp suppresses the aberrant accumulation of IP_3R1 and pan-RYR but not PS1 proteins (Fig. 5D; Supplementary Material, Fig. S4B). Neither knockdown nor ectopic expression of Herp alters mRNA levels of IP_3R1 and pan-RYR (Supplementary Material, Fig. S4C and D), suggesting that Herp promotes the homeostatic regulation of these ER-resident Ca^{2+} release channels through a mechanism that is independent of transcription.

Knockdown of Herp also increases basal (Fig. 5E and F) and stress-induced accumulation (Fig. 5E and G) of both IP_3R1 and pan-RYR proteins independently of transcription (Fig. 5H) in PC12-Tuni. Consistent with the notion that Herp counteracts Tuni-induced death (19), knockdown of Herp results in a significant increase in the CHOP protein by transcriptional regulation (Fig. 5E and H).

Herp promotes degradation of ER-resident Ca^{2+} release channels through ERAD

Because Herp has been shown to bind to and target protein substrates for ERAD (17), we next tested whether Herp modulates the levels of IP_3R1 and/or pan-RYR proteins by a similar mechanism. Immunoprecipitation with an anti-Herp antibody followed by immunoblotting with antibodies to each ER Ca^{2+} release channel demonstrated that a greater fraction of Herp forms a complex with IP_3R1 and pan-RYR in PC12-Tuni when compared with vehicle-treated control cells (Fig. 6A). The specificity of the interaction was confirmed by immunoblotting the Herp-containing protein complex with an antibody to Grp78 (Supplementary Material, Fig. S5A) and by performing the co-immunoprecipitation assay using lysates from human embryonic kidney 293 (HEK293) expressing c-myc-tagged Herp (Supplementary Material, Fig. S5B). Neither the pre-immune normal IgG nor Grp78 antibody forms a protein complex with Herp. Double immunofluorescence labeling confirmed Herp colocalization with each ER Ca^{2+} release channel protein in PC12-Tuni (Supplementary Material, Fig. S5C). Herp also interacts with A53TαSyn (Supplementary Material, Fig. S5D and E), suggesting that this interaction could possibly interfere with the protective role of Herp (see Discussion).

To determine whether binding of Herp to IP_3R1 and pan-RYR results in proteasome-mediated protein degradation of these ER Ca^{2+} release channel proteins, PC12 cells were treated with the proteasome inhibitor MG-132. Consistent with the notion that the degradation of IP_3R1 and pan-RYR proteins is mediated by the proteasomes (27,28), MG-132 markedly increases steady-state protein levels of these ER-resident Ca^{2+} release channels (Fig. 6B; Supplementary Material, Fig. S6A). Ectopic expression of Herp results in a significant reduction in IP_3R1 and pan-RYR protein levels that can be reversed upon inhibition of proteasome activity (Fig. 6C, Supplementary Material, Fig. S6B). In contrast, expression of ΔUBL-Herp failed to induce a significant decrease in the levels of these ER Ca^{2+} release channel proteins (Fig. 6D).

Note that MG-132 also increases Herp protein levels (Fig. 6B and C), suggesting that Herp itself is a proteasome substrate (29). In support for this notion, Herp interacts and co-localizes with the ubiquitin-interacting S5a subunit of the proteasome in PC12-Tuni (Supplementary Material, Fig. S7A and B). Increased co-localization of S5a with the Grp78-labeled ER was also detected in PC12 cells transfected with Herp (Supplementary Material, Fig. S7B). Although the S5a protein level was not markedly altered in PC12-Tuni (Supplementary Material, Fig. S7C), knockdown of Herp substantially reduces S5a co-localization with the ER in PC12-Tuni, suggesting that ER stress-induced upregulation of Herp but not S5a is sufficient for the recruitment of proteasomes to the ER (Supplementary Material, Fig. S7D). Consequently, Herp knockdown also results in a marked decrease in the steady-state level of the ubiquitinylated IP3R1 protein (Fig. 6E). Collectively, our data indicate that aberrant accumulation of IP_3R and pan-RYR perturbs ER Ca^{2+} homeostasis in ER-stressed cells and that Herp prevents aberrant ER Ca^{2+} release by targeting these ER-resident Ca^{2+} release channels for ERAD.

Accumulation of ER stress markers and ER-resident Ca^{2+} channels in A53TαSyn transgenic mice

Next, we explored whether A53TαSyn-induced ER stress markers and ER Ca^{2+} channels were detected *in vivo*. Transgenic mice overexpressing A53TαSyn (A53T mice) develop motor abnormalities associated with the accumulation of αSyn inclusions in spinal cord motor neurons (30). Immunoblotting reveals marked upregulation of Herp and Grp78/Bip proteins in spinal cords of ≥8-month-old A53T mice (symptomatic) when compared with 2-month-old A53T mice (pre-symptomatic) and non-transgenic (non-Tg) mice (Fig. 7A and B). The CHOP protein was low in non-Tg mice but was readily detected in A53T mice (Fig. 7A and B). Immunohistochemistry indicates a marked increase in nitrated αSyn in NeuN-labeled spinal cord neurons and further confirms the increase in ER stress markers and ER-resident Ca^{2+} release channels in 13–15-month-old (symptomatic) when compared with 5-month-old (pre-symptomatic) A53T mice (Supplementary Material, Fig. S8A). In contrast to the ER stress markers, the upregulation of ER-resident Ca^{2+} release channels was not attributed to increased expression (Supplementary Material, Fig. S8B). The amounts of IP_3R1 and pan-RYR in the spinal cord homogenates that form a protein complex with Herp were also markedly higher in A53T compared with non-Tg mice (Fig. 7C and D) consistent with the notion that ERAD may contribute to the homeostatic regulation of ER Ca^{2+} release channel proteins in spinal cord motor neurons. The interaction between Herp and A53TαSyn was also confirmed in spinal cords of symptomatic transgenic mice (Supplementary Material, Fig. S8C), suggesting that this interaction may impair the ability of Herp to prevent the aberrant accumulation of ER-resident Ca^{2+} release channels and, hence, its ER Ca^{2+}-stabilizing action in ER stressed motor neurons. These findings link aberrant ER Ca^{2+} regulation and chronic ER stress to motor neuron dysfunction and death in the pathophysiology of synucleinopathies.

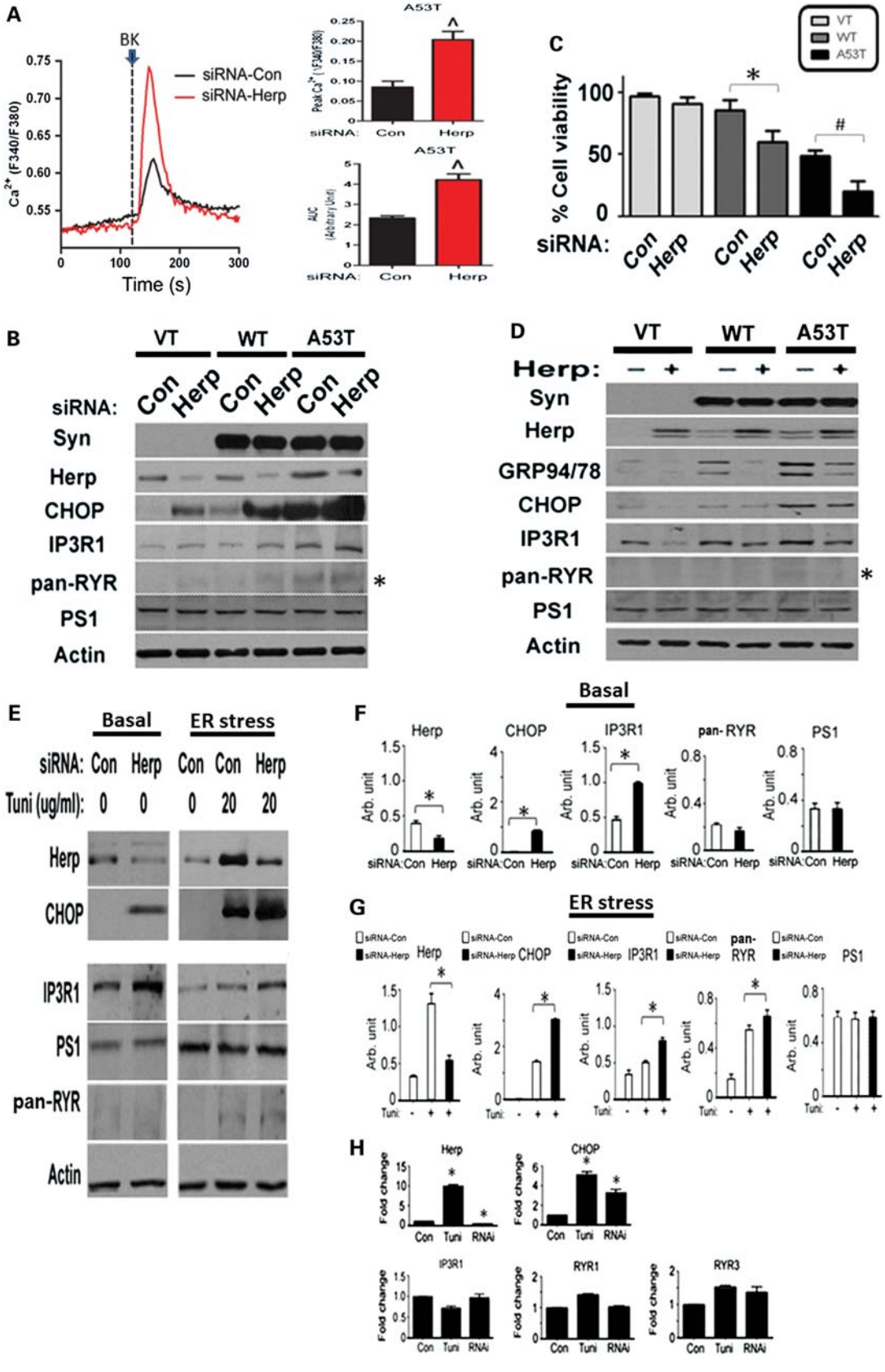
A
BK
siRNA-Con
siRNA-Herp
Ca2+ (F340/F380)
Time (s)
A53T
Peak Ca2+ (F340/F380)
AUC (Arbitrary Unit)
siRNA: Con Herp
B
VT WT A53T
siRNA: Con Herp Con Herp Con Herp
Syn
Herp
CHOP
IP3R1
pan-RYR
PS1
Actin
C
VT
WT
A53T
% Cell viability
siRNA: Con Herp Con Herp Con Herp
D
VT WT A53T
Herp: – + – + – +
Syn
Herp
GRP94/78
CHOP
IP3R1
pan-RYR
PS1
Actin
E
Basal
ER stress
siRNA: Con Herp Con Con Herp
Tuni (ug/ml): 0 0 0 20 20
Herp
CHOP
IP3R1
PS1
pan-RYR
Actin
F
Basal
Herp
CHOP
IP3R1
pan- RYR
PS1
Arb. unit
siRNA:Con Herp
G
ER stress
siRNA-Con
siRNA-Herp
Herp
CHOP
IP3R1
pan-RYR
PS1
Arb. unit
Tuni: - + +
H
Herp
CHOP
IP3R1
RYR1
RYR3
Fold change
Con Tuni RNAi

DISCUSSION

Neuronal loss in both familial and sporadic forms of neurodegenerative disorders is accompanied by formation of protein inclusions or fibrillar aggregates composed of misfolded proteins that can induce ER stress. The accumulation of evidence that ER stress is critically involved in the pathogenesis of neurodegenerative disorders suggests that approaches that aim to halt ER stress may prevent the pathological cascades induced by protein inclusions. There is growing evidence that the ER can play pivotal roles in regulating cell survival and apoptosis in a variety of cell types, including neurons (30,31), but the mechanisms linking ER stress to apoptosis are incompletely understood. The identification of conditions that slow ER stress may reveal novel strategies for counteracting ER stress-mediated cell death.

The ER is the major intracellular store of Ca^{2+} and aberrant regulation of luminal ER Ca^{2+} is thought to play critical roles in many apoptotic cascades (31). Deregulated ER Ca^{2+} homeostasis has also been implicated in the pathophysiology of chronic neurodegenerative diseases, such as prion disorders, Huntington's and Alzheimer's (32–34). Here we showed that A53TαSyn evokes ER stress and that the attendant disturbances in ER Ca^{2+} homeostasis contributes to a higher sensitivity to ER stress-induced cell death. We demonstrate that Herp counteracts A53TαSyn-induced cell death by stabilizing ER Ca^{2+} homeostasis. Ectopic expression of Herp markedly reduced A53TαSyn-induced toxicity, whereas knockdown of Herp exacerbates or prolongs ER stress leading to a significant augmentation of toxicity. Hence, a better understanding of the function of Herp is therefore of high significance to elucidate the functional link between the ER stress and ER Ca^{2+} homeostasis and to develop mechanism-based neuroprotective strategies for PD and related neurodegenerative diseases.

The underlying molecular mechanism(s) whereby Herp modulates ER Ca^{2+} homeostasis remains poorly understood. Knockdown of Herp leads to the accumulation of IP_3R1 and pan-RyR proteins in PC12 cells and, consequently, promotes aberrant ER Ca^{2+} release that in turn may decrease the threshold for the activation of ER stress-related cell death pathways. Consistent with this notion, gene knockdown and pharmacological inhibition of ER Ca^{2+} release channels ameliorates ER stress and protects PC12-A53TαSyn and PC12-Tuni against ER stress-induced cell death (Fig. 4). Conversely, overexpression of Herp stabilizes ER Ca^{2+} homeostasis and inhibits ER stress-induced cell death by preventing the accumulation of ER Ca^{2+} release channel proteins in PC12-A53TαSyn. It is noteworthy that the accumulation of IP_3R1 and pan-RyR proteins was partially suppressed in spite of the elevated level of endogenous Herp in PC12-A53TαSyn, suggesting that binding of Herp to A53TαSyn (Supplementary Material, Fig. S5D and E) and its accumulation in the core of Lewy bodies (18) may interfere with its protective function and that ectopically expressed Herp can overcome this A53TαSyn-mediated inhibition.

A recent study by Higo *et al*. (35) reported that various ER stressors disrupt IP3R1 channel activity by impairing its tetrameric assembly. At the molecular level, the interaction of IP3R with Grp78, a chaperone that is critical for the assembly of functional IP3R complexes, was inhibited during ER stress. It is noteworthy that the inhibition of IP3R1-tetrameric assembly and IP3R1-mediated Ca^{2+} release can be prevented by ectopic expression of Grp78 (35). Hence, we proposed that cell-type-specific regulation of the ER stress response which determines the expression level of Grp78 and, consequently, the susceptibility to the disruption of IP3R1 channel activity may be responsible for the observed discrepancy. Alternatively, we cannot exclude the possibility that a molecule that targets the interaction between Grp78 and IP3R1 may be induced in a dose or cell-type-specific manner during ER stress.

Higo *et al*. (35) also reported that knockdown of IP3R1 in Purkinje neurons and HeLa cells, both cell types that predominantly express IP3R1, resulted in enhanced vulnerability to ER stress-induced death. In their study, the expression of IP3R1 was abrogated by RNA interference for 48 h. As IP3R-mediated Ca^{2+} signaling is vital for processes important for survival, such as transcription, proliferation and plasticity, impaired IP3R1 function is likely to increase vulnerability to a low dose of the ER stressor. Using the same knockdown approach for 8 and 24 h, we were able to effectively suppress the ER stress-induced accumulation of IP3R1 without causing a significant reduction in the basal level of this ER Ca^{2+} release channel (Supplementary Material, Fig. S2).

Mechanistically, Herp interacts with and facilitates the degradation of ER Ca^{2+} release channel proteins by ERAD. Several recent studies support a role for Herp in ERAD (17) based on the notion that Herp is rapidly degraded in a

Figure 5. Herp stabilizes Ca^{2+} homeostasis by preventing ER stress-induced accumulation of ER-resident Ca^{2+} release channels. (**A**) Representative recordings of the BK-evoked increase in intracellular Ca^{2+} ($[Ca^{2+}]i$) in PC12 cells expressing mutant (A53T) αSyn 24 h after transfection with siRNA-Con or siRNA-Herp (100 nM). Arrow indicates the time of BK addition. Cells were loaded with fura-2 and $[Ca^{2+}]_i$ was recorded in Ca^{2+}-free medium as described under 'Materials and Methods'. Histograms show Ca^{2+} peak values (change from baseline) and AUC. Values are the mean ± SEM of determinations made in four to six separate cultures (15–20 cells assessed/culture). $^{\wedge}P < 0.001$, compared with siRNA-Con. (**B**) Representative immunoblots of ER stress proteins and Ca^{2+} release channels in PC12 cells expressing VT, WT or A53T 24 h after transfection with siRNA-Con and siRNA-Herp (100 nM). Asterisk indicates the protein band corresponding to pan-RYR. The level of actin is not affected by siRNA treatment. (**C**) Histograms showing the viability of PC12 cells expressing VT, WT or A53T 24 h after transfection with siRNA-Con or siRNA-Herp (100 nM). Values represent the mean ± SEM of three independent experiments. $^{\#}P < 0.05$; $^{*}P < 0.01$, compared with the siRNA-Con-treated groups. (**D**) Representative immunoblots of levels of ER stress proteins and Ca^{2+} release channels in PC12 cells expressing VT, WT or A53T after transfection with empty vector (−) or vector expressing Herp (+) for 48 h. Asterisk indicates the protein band corresponding to pan-RYR. (**E**–**G**) Representative immunoblots and results of densitometric analysis of the indicated protein levels in PC12 cells that were either transfected with the indicated siRNAs and collected 24 h after (basal condition; left panels) or transfected with the siRNAs 8 h prior to incubation with Tuni (20 μg/ml) for 24 h (ER stress condition; right panels). $^{*}P < 0.01$, compared with the siRNA-Con-treated groups. (**H**) qRT-PCR analysis of the relative expression of the indicated proteins in PC12 cells that were treated with vehicle control (Con), Tuni (20 μg/ml) or siRNA-Herp (100 nM) for 24 h. Values represent the mean ± SEM of three independent experiments. The mRNA level in Con was set at 1. $^{*}P < 0.01$, compared with Con.

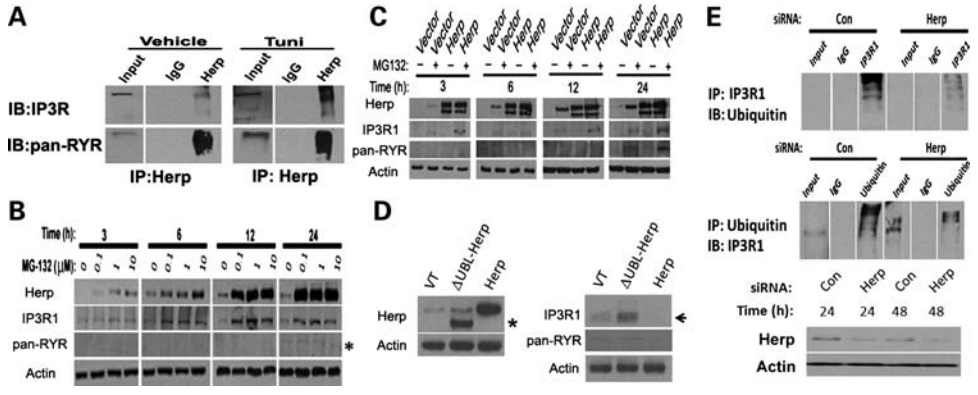

Figure 6. Herp interacts with and facilitates proteasomal-mediated degradation of ER-resident Ca2+ release channels. (**A**) Representative immunoblots of the indicated ER Ca^{2+} release channels immunoprecipitated (IP) by anti-Herp antibody from lysates of PC12 that were treated with either Tuni (20 μg/ml) or vehicle for 16 h. The pre-immune normal IgG used as the negative control failed to yield an immunopositive band for IP3R or RYR. Input verifies the presence of these ER Ca^{2+} release channel protein in cell lysates. (**B**) Representative immunoblots of Herp, IP3R1 and pan-RYR protein levels in PC12 cells that were treated with the indicated doses of the proteasomal inhibitor MG-132 for 3, 6, 12 and 24 h. (**C**) Representative immunoblots of Herp, IP_3R and pan-RYR protein levels in PC12 cells that were transfected with either an empty plasmid (Vector) or a plasmid expressing Herp 24 h prior to the addition of 1 μM MG-132. Cells were collected at the indicated time points after MG-132 addition. (**D**) Representative immunoblots of Herp, IP3R1 and pan-RYR protein levels in PC12 cells after transfection with the empty vector (VT) or a vector expressing either Herp or ΔUBL-Herp. Cells were collected at 24 h. Blots were reprobed for actin to confirm equality of total protein loading. The ΔUBL-Herp and IP3R1 protein bands are indicated by the asterisk and arrowhead, respectively. (**E**) Representative immunoblots of the levels of ubiquitinylated IP3R1 in lysates of PC12 that were treated with siRNA-Con or siRNA-Herp (100 nM) for 24 h. Levels of the ubiquitinylated IP3R1 protein were assessed by immunoprecipitation (IP) with the anti-IP3R1 antibody and immunoblotted (IB) with the anti-ubiquitin antibody (top) and, conversely, by IP with the anti-ubiquitin antibody and IB with the anti-IP3R1 antibody (center). The pre-immune normal IgG used as the negative control failed to yield an immunopositive band for IP3R1. Input verifies the presence of IP3R1 in cell lysates. Knockdown of Herp was confirmed by immunoblotting (bottom).

proteasome-dependent fashion (29) and that knockdown of Herp leads to the accumulation of several established ERAD substrates (17). Herp has been shown to interact with Hrd1, a membrane-anchored E3 ligase that is required for ERAD (17), and with ubiquilin, a shuttle protein that delivers ubiquitinated substrates to the proteasome for degradation (36). We found that Herp knockdown in ER stressed cells leads to the accumulation of both IP_3R1 and pan-RYR proteins. Conversely, ectopic expression of Herp prevents the accumulation of these ER Ca^{2+} release channels. Treatment with MG-132 not only elevates basal levels of IP_3R1 and pan-RYR proteins but also prevents the ability of Herp to suppress their accumulation in ER stressed cells (Fig. 6B and C), suggesting the critical involvement of ERAD in the homeostatic regulation of these ER Ca^{2+} release channels. Deletion and function analyses further support the involvement of ERAD in Herp-mediated cell protection via the stabilization of ER Ca^{2+} homeostasis. Ectopic expression of Herp lacking the UBL domain that is essential for the efficient degradation of ERAD substrates (17,36) fails not only to stabilize ER Ca^{2+} homeostasis but also to protect PC12-Tuni (16) and PC12-A53TαSyn from ER stress-induced death (Fig. 2E). The potentiation of A53TαSyn-induced cell death following ectopic expression of ΔUBL-Herp may be related to the aberrant accumulation of IP_3R1 and pan-RYR proteins (Fig. 6D).

It is noteworthy that Miura *et al*. (37) showed that Herp KO cells were resistant to proteolytic stress resulting from the inhibition of proteasomes, suggesting that the protective action of Herp may be related to the types of cellular stress. The accumulation of two cytosolic proteins, including αSyn and synphilin-1, was markedly lower in F9 Herp KO cells when compared with wild-type control cells, indicating that Herp may retard the degradation of these cytosolic proteins whose accumulation may result in enhanced vulnerability to proteolytic stress-induced death. Whether knockdown of Herp may improve the viability of PC12-A53TαSyn under proteolytic stress was not investigated in this study. These data suggest that modulation of Herp can differentially impact the turnover of ER and cytosolic proteins and, consequently, the cell fate that is dependent on the type of cellular stress.

Our data provide the first evidence that ER stress is regulated by the activity of ER-resident Ca^{2+} release channels. We found that pharmacological inhibition or knockdown of ER Ca^{2+} release proteins ameliorates ER stress-induced cell death, suggesting that the aberrant ER Ca^{2+} release is associated with higher susceptibility to chronic enhancement of ER stress. Though the detailed mechanisms underlying Ca^{2+}-dependent cell death in PC12-A53TαSyn was not investigated in the present study, it is likely that accumulation of ER Ca^{2+} release channels leads to enhanced ER to mitochondria Ca^{2+} flow that triggers the loss of mitochondrial membrane potential and increased generation of reactive oxygen species (ROS) (16). Previous studies demonstrate that ROS-induced damage to the ER may amplify Ca^{2+} release via a mechanism involving oxidation-induced activation of RYR and IP_3R (38). Ectopic expression of Herp has been shown to counteract this deleterious positive feedback loop by inhibiting the proapoptotic Ca^{2+} flow from the ER to mitochondria in PC12 cells exposed to the PD-inducing toxin 1-methyl-4-phenylpyridinium (MPP^+) (19). The increase in CHOP detected in PC12-Tuni, PC12-A53TαSyn and siRNA-Herp-treated PC12 cells likely results from the depletion of ER Ca^{2+} store associated with the aberrant accumulation of IP_3R1 and pan-RYR as ectopic expression of Herp counteracts CHOP upregulation by promoting the homeostatic regulation of these ER Ca^{2+} channel proteins.

It is noteworthy that chronic enhancement of ER stress resulting from the disruption of ER Ca^{2+} homeostasis could

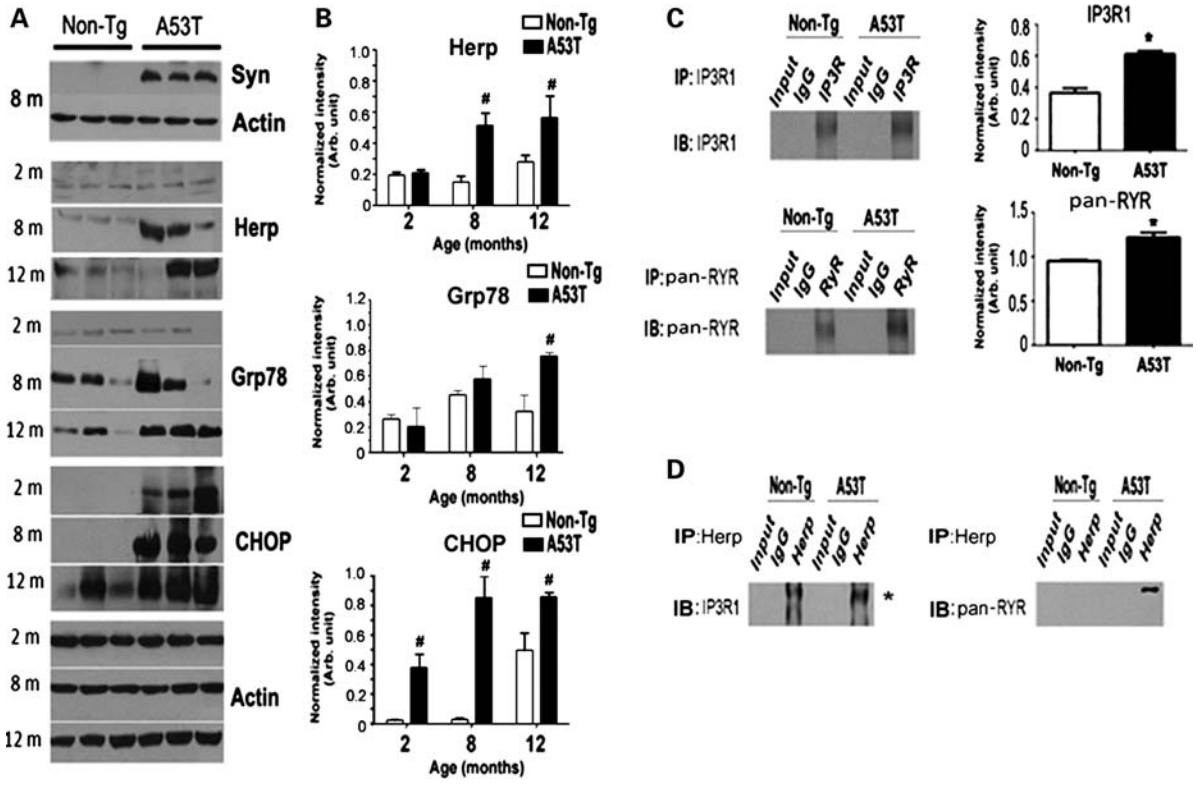

Figure 7. Elevation of ER stress markers and ER-resident Ca2+ release channels in A53T-αSyn mice. (**A** and **B**) Representative immunoblots (A) and results of densitometric analysis (B) of the indicated ER stress proteins in lumbar spinal cords from age-matched non-Tg and mutant αSyn (A53T) mice. A representative immunoblot confirming the expression of human αSyn in spinal cords of A53T is shown (upper panel). All immunoblots were reprobed for actin to control for equal protein loading (bottom panels). Values represent the mean ± SEM of four mice per group. $^{\#}P < 0.05$; $^{*}P < 0.01$, compared with non-Tg mice. (**C**) Immunoprecipitation to quantify protein levels of IP3R1 (top) and pan-RYR (bottom) in lumbar spinal cords of 8-month-old non-Tg and A53T mice. Each ER Ca^{2+} release channel protein was immunoprecipitated (IP) and immunoblotted (IB) with the respective antibodies. Pre-immune normal IgG was used as a negative control for IP. Histograms show the densitometric analysis of the band corresponding to each ER Ca^{2+} release channel protein. Values represent the mean ± SEM of four mice per group.$^{*}P < 0.01$ compared with non-Tg mice. (**D**) Representative immunoblots of IP_3R1 (left) and pan-RYR (right) in protein complexes IP with anti-Herp antibody from lumbar spinal cord homogenates of 8-month-old non-Tg and A53T mice. Pre-immune normal IgG was used as a negative control for IP. Asterisk denotes the specific band.

trigger αSyn protein aggregation in the cytosol and that blockade of ER Ca^{2+} release channels (Supplementary Material, Fig. S2) ameliorates αSyn inclusion formation suggesting a causative link between chronic ER stress and αSyn oligomer formation. Consistent with this notion, sustained ER Ca^{2+} release triggered by thapsigargin accelerates the formation of potentially cytotoxic oligomers in αSyn-EGFP transfected cells (26). Tuni at doses that induce chronic stress associated with sustained ER Ca^{2+} release (16,39) has also been shown to promote the accumulation of αSyn oligomers (40). Consistent with the findings in PC12-A53T cells, we detected higher levels of several ER stress markers, including the ER stress-induced apoptotic mediator CHOP, and ER-resident Ca^{2+} release channels in the spinal cords of symptomatic A53T mice when compared with non-Tg and pre-symptomatic A53T mice, suggesting that accumulation of A53TαSyn promotes motor neuron degeneration in part by a mechanism involving chronic ER stress associated with the deregulation of ER Ca^{2+} homeostasis. In addition to the elevation of the Herp protein, we detected increased interaction of Herp with A53TαSyn in spinal cord homogenates of symptomatic A53T mice which further supports the notion that Herp-dependent ERAD of ER-resident Ca^{2+} release channels may be impaired in vulnerable motor neurons.

DA neurons appear to be relatively resistant to degeneration in A53T mice (30,41) and express relatively high levels of the Ca^{2+}-binding protein calbindin (41). In contrast, spinal cord motor neurons are characterized by low cytosolic Ca^{2+} buffering capacities (41) and, hence, may be more susceptible to chronic ER stress induced by A53TαSyn and associated degenerative processes triggered by the aberrant ER Ca^{2+} release. Future studies will determine whether direct modulation of Herp expression *in vivo* may impact the levels of ER-resident Ca^{2+} release channel proteins, αSyn inclusion formation, disease manifestations and progression. Because ER stress elicited by the aggregation of amyotrophic lateral sclerosis-linked mutant superoxide dismutase 1 has been implicated in motor neuron death (42,43), elucidation of the cellular and molecular mechanisms that promote or prevent disturbances in ER Ca^{2+} homeostasis may lead to novel approaches for therapeutic intervention for synucleinopathies and motor neuron diseases.

MATERIALS AND METHODS

Cells, plasmid and reagents

PC12 and HEK293 cells were purchased from ATTC. PC12 cells were selected because they are DA and have been extensively studied as models of neuronal degeneration. The pcDNA3.1 plasmids containing the c-myc-tagged full-length or loss-of-function deletion of human Herp cDNA have been described previously (16,19). Xestospongin C (Tocris), dantrolene (Sigma) and BK (Sigma) were prepared as concentrated $\times 1000$ stocks in dimethylsulfoxide (DMSO; Sigma) or Lock's solution (mM): NaCl, 154; KCl, 5.6; $CaCl_2$, 2.3; $MgCl_2$, 1.0; $NaHCO_3$, 3.6; glucose, 10; Hepes buffer, 5 (pH 7.2). The dose of each drug was selected based on previously published studies (11,20). Caffeine (Sigma) was freshly prepared in water. Additional reagents included: Lipofectamine 2000, TRIzol, Opti-MEM, priopidium iodide, and protein A beads (Invitrogen), MG-132 (BioMol), Trypan blue solution (0.4%; VWR) and Tuni (Sigma).

Cell culture, transduction and electroporations

PC12 and HEK293 cells were maintained in a humidified 5% CO_2 and 95% air atmosphere at 37°C in Dulbecco's modified Eagle medium (DMEM) high glucose medium supplemented with 10% heat-inactivated horse serum, 5% heat-inactivated fetal bovine serum, 50 units/ml penicillin and 0.05 mg/ml streptomycin (16,20). PC12 cell lines expressing the human wild-type and mutant αSyn were generated using a Tet-on system. For the induction of αSyn expression, the culture medium was replaced every other day with DMEM containing 1% horse and 0.5% fetal bovine sera (InVitrogen), 100 ng/ml nerve growth factor (Upstate) and Tet (2 μM; Sigma). In some studies, non-induced clones were transduced with recombinant adeno-associated viral (rAAV) particles prior to induction with Tet. Transient transfection was carried out using the Neon transfection system according to the manufacture's instructions (Invitrogen). PC12 cells ($1-2 \times 10^7$/ml) were transfected by electroporation with 4–8 μg of empty vector, wild-type αSyn or mutant αSyn (gift from Dr R.G. Perez, Department of Neurology, University of Pittsburgh) using the following optimized conditions: 1400 V, 20 ms and 1 pulse. The transfection efficiency following electroporation with wild-type αSyn-EGFP was ~70%.

Ectopic expression of Herp

The Herp and ΔUBL-Herp constructs have been inserted into a rAAV expression construct (GenDetect). The resulting cDNAs were cloned into the *Hin*dIII/*Bam*HI site of the pAd-YC2 shuttle vector. For homologous recombination, the shuttle vector (5 μg) and rescue vector pJM17 (5 μg) were co-transfected into HEK293 cells. To amplify the recombinants, cell culture supernatant was serially diluted into serum-free media and incubated with HEK293 cells. The recombinants were purified from supernatants by ultracentrifugation. The band containing mature viral particles was collected and desalted against phosphate-buffered saline (PBS) in a Vivaspin column (Vivascience AG), and titers were determined by counting the number of plaques. Cells were infected with the virus at a multiplicity of infection of 500 in the medium containing 2% fetal bovine serum (FBS) for 4 h, after which DMEM containing 10% FBS was added. Analysis of rAAV-GFP expression indicated an infection rate of ~85–90%.

Experimental treatments

To induce ER stress, cultures of PC12 cells were treated with 20 μg/ml Tuni. In some studies, the proteasomal inhibitor MG-132 (0.1–10 μM) was added prior to Tuni. These drugs were prepared in DMSO immediately before applying them to the cultures. When DMSO was used as the solvent, their final concentration did not exceed 0.1%. At the end of each treatment, the cultures were processed for immunoblotting and evaluating cell viability.

RNA interference

Cells were transfected with Mission predesigned siRNA duplexes (Sigma) targeting Herp, IP_3R1, RYR1 and RYR3, or a control siRNA (siRNA-Con; Ambion) using Lipofectamine 2000 (Invitrogen) in Opti-MEM according to the manufacturer's protocol. The target sequences of each siRNA are listed in Supplementary Material, Tables S1. Results of qRT-PCR analysis of total RNA from PC12 cells and tissue samples revealed expression of IP_3R2, IP_3R3 and RYR2 below the limit of detection of the qRT-PCR assay method (Ct values > 35). The optimized siRNA concentrations are 100 nM of siRNA-Herp, 250 nM of siRNA-IP_3R1 and 100 nM of each siRNA-RYR1 and siRNA-RYR3 added in combination. After 4 h of transfection, the medium was replaced, and 24–48 h later, the indicated experiments were conducted. To monitor knockdown, cells were harvested and processed for qRT-PCR and western blot analyses. The transfection efficiency of siRNA-Con-fluorescein isothiocyanate (FITC) (Santa Cruz) in PC12 cells was >95% (data not shown).

Assessment of cell death

Cell death was assessed by either trypan blue exclusion or propidium iodide staining as described previously (16,20). Trypan blue and propidium iodide (50 μg/ml) stain only the cells with disrupted plasma membrane integrity so these cells were considered dead. The PI was excited with the 568 nm yellow line of a confocal microscope (Leica), and the acquisition of PI labeling images was performed at the wavelength >600 nm via a photomultiplier through a band-pass filter centered at 605 nm. Dead cells were counted in four microscopic fields per dish, with a minimum of 100 cells per field and results were expressed as a percentage of the total number of cells. All of the experiments were repeated at least three times without the knowledge of treatment history.

Immunoprecipitation

Cells and tissues were solubilized in binding buffer containing 50 mM Tris–HCl (pH 7.4), 150 mM NaCl, 1 mM EDTA, 1 mM DTT, 0.2 mM phenylmethanesulfonyl fluoride and 1.0% NP-40 as described previously (21). The homogenate was centrifuged

at 20 000*g* for 10 min. Solubilized proteins were adjusted to 0.1% NP-40 and incubated for 12 h at 4°C with a polyclonal antibody to anti-Herp (BioMol), IP3R1 (Millipore) or pan-RyR (Santa Cruz). After an additional incubation with protein A-conjugated beads, the immune complexes were then recovered by low speed centrifugation and washed extensively with the binding buffer containing 0.1% NP-40. Immunoprecipitated proteins were eluted by boiling in sodium dodecyl sulfate polyacrylamide gel electrophoresis (SDS-PAGE) sampling buffer and analyzed by immunoblotting.

Immunoblotting

Protein lysates were centrifuged at 20,000 g and equal amounts of the proteins were loaded into each well of a SDS–PAGE. After electrophoretic separation and transfer to nitrocellulose membranes (Bio-rad), blots were incubated in blocking solution (5% milk in TBS-T) for 1 h at RT, followed by an overnight incubation with primary the following antibodies diluted in blocking buffer: α-Syn [human specific antibody (Abcam) or cross-reactive with human, rat, and mouse (Santa Cruz)], KDEL (Santa Cruz), actin (Sigma), ERK1 (Cell Signaling), Casp12 (Abcam), Herp [polyclonal antibody (Biomol) and monoconal antibody (Santa Cruz)], CHOP (Abcam), IP3R1 (Millipore), pan-RyR (Santa Cruz), S5a (Cell Signaling) and presenilin 1 (Abcam). Membranes were then incubated for 1 h in secondary antibody conjugated to horseradish peroxidase, and bands were visualized by enhanced chemiluminescence (Thermo-Scientific). Membranes were stripped and re-probed with either the actin or ERK1 antibody to normalize protein loading. The intensity of the signals obtained was quantified by densitometric scanning using Scion (NIH Image).

Immunostaining

Spinal cords were removed after perfusion with heparinized saline (0.9% NaCl) transcardially followed by 4% buffered paraformaldehyde (PFA) and post-fixed overnight in PFA. Serial sections of the lumbar region were sectioned at 30 μm with a freezing microtome (Microm HM 505 N) and collected on slides. Cultured cells plated on cover slips were fixed for 20 min with 4% PFA in PBS following experimental treatments. Cells were then incubated for 5 min in a solution of 0.2% Triton X-100 in PBS and for 1 h in blocking solution (0.02% Triton X-100, 5% normal horse or goat serum in PBS). Tissue sections and cover slips were processed for immunofluorescence staining as described (16,21) with the following primary antibodies: αSyn (Abcam), nitro-αSyn (Abcam), Herp (Santa Cruz); CHOP (Cell Signaling); KDEL (Santa Cruz); pan-RyR (Santa Cruz), IP3R1 (Millipore) and NeuN (Millipore). All antibodies were diluted in blocking solution and used within the concentration ranges recommended by the manufacturer. To test for non-specific staining by the secondary antibodies, additional sections or cover slips were processed in a similar fashion without the primary antibodies or with adsorbed antibodies. After three washes, sections or cover slips were incubated with FITC-conjugated anti-rabbit and Cy3-conjugated anti-mouse secondary antibodies and then mounted. To stain the nuclei, sections or cover slips were further incubated with the nucleic acid stain 4′,6-diamidino-2-phenylindole in PBS containing 1% RNase and 0.2% Triton X-100 for 10 min, and then mounted in Fluor-Save aqueous mounting medium (Calbiochem). Immunofluorescence staining was examined by using a NIKON 80i fluorescent microscope equipped with a ×60 oil immersion objective lens. For quantification, digitized images of immunostained sections were obtained with Qimaging Retiga 2000 SVGA FAST 1394 cooled digital camera system mounted on the microscope and then analyzed with IP lab software (BD Biosciences Bioimaging). Total area of pixel intensity was measured with the automated measurement tools in the IP lab software. The total density was averaged and expressed as normalized, corrected values.

Measurement of $[Ca^{2+}]i$

PC12 cells were plated at a density of 1×10^6 cells/35 mm glass bottom MatTek dish (Ashland) the day before the experiment. Cells were loaded with 2 μM Fura-2 acetoxymethyl ester in Krebs–Ringer–Hepes (KRH) buffer [129 mM NaCl, 5 mM $NaHCO_3$, 4.8 mM KCl, 1.2 mM KH_2PO_4, 1 mM $CaCl_2$, 1.2 mM $MgCl_2$, 10 mM glucose and 10 mM Hepes (pH 7.4)], for 20 min and then washed twice with KRH and incubated for additional 30 min at 37°C. Dishes were placed into a heated chamber mounted on the stage of an inverted fluorescence microscope (Nikon Eclipse TiE with perfect focus and DG-5 Xenon excitation) and perfused with Ca^{2+}-deficient KRH at a rate of 1.5 ml/min. Baseline was established for 6 min before stimulation. Measurements were continued for 4–5 min after Ca^{2+} peak was recorded. Fura-2 dual excitation images were captured through a Nikon S Fluor ×20 objective (NA 0.75) with a Photometrics QuantEM 16 bit EMCCD camera using 340 and 380 nm excitation filters and a 470–550 nm emission filter. Data were acquired and analyzed using Nikon Elements software. Background fluorescence signals were collected at the same rate for the same wavelengths and were subtracted from the corresponding fluorescence images. The fluorescence intensities of 10–20 cells/dish were expressed as ratio of excitation 340/380 nm and area under the curve (AUC).

RT-PCR and qRT-PCR

Total RNA was isolated with TRIzol (Invitrogen). To prevent genomic DNA contamination, the isolated total RNA samples were treated with DNAse. Two micrograms of total RNA was reverse transcribed with Superscript II reverse transcriptase and an oligo(dT) primer (Invitrogen). RT-PCR products were resolved on agorose gels stained with ethidium bromide. Relative quantification of gene expression was performed by normalizing the fluorescence intensities of each band to those of actin. qRT-PCR was performed as previously described (22). The integrity of the RT-PCR products was confirmed by melting curve analysis. Melting curves for all reaction showed one specific peak. We used 18 S rRNA as an endogenous control to normalize variations in RNA extraction and variability in RT efficiency. mRNA levels were quantified with the comparative C_t method (22). The pairs of primers

used for RT-PCR and qRT-PCR are listed in Supplementary Material, Tables S2 and S3, respectively.

Animals

Mice transgenic for human A53Tα-Syn (THY1-SNCA-A53T; Jackson) have been characterized in a previous study (30). All animal experimental procedures were performed in accordance with the guidelines of the NIH and approved by the Institutional Animal Care and Use Committee at University of Central Florida.

Statistical analysis

Comparison between two groups was performed using Student's *t*-test, whereas multiple comparisons between more than two groups were analyzed by one-way analysis of variance (ANOVA) and *post hoc* tests by least significant difference. Data evaluated for the effects of two variables was analyzed using two-way ANOVA (Prism 4 version 4.03; GraphPad Software, Inc.). Results are presented as means ± SEM. For all analyses, statistical significance is defined as a P value ≤ 0.05.

SUPPLEMENTARY MATERIAL

Supplementary Material is available at *HMG* online.

ACKNOWLEDGEMENTS

We are grateful to Binbin Yan for technical assistance with confocal microscopy.

Conflict of Interest statement. None declared.

FUNDING

This work was supported by the American Federation on Aging Research (to S.L.C.); National Institutes of Health (NIH 1R21NS066265-01 to S.L.C.); and the National Institute on Aging Intramural Research Program of the National Institute of Health (to M.P.M.).

REFERENCES

1. Spillantini, M.G., Crowther, R.A., Jakes, R., Hasegawa, M. and Goedert, M. (1998) Alpha-synuclein in filamentous inclusions of Lewy bodies from Parkinson's disease and dementia with lewy bodies. *Proc. Natl Acad. Sci. USA*, **95**, 469–473.
2. Conway, K.A., Harper, J.D. and Lansbury, P.T. (1998) Accelerated in vitro fibril formation by a mutant alpha-synuclein linked to early-onset Parkinson disease. *Nat. Med.*, **4**, 1318–1320.
3. Singleton, A.B., Farrer, M., Johnson, J., Singleton, A., Hague, S., Kachergus, J., Hulihan, M., Peuralinna, T., Dutra, A., Nussbaum, R. *et al.* (2003) Alpha-synuclein locus triplication causes Parkinson's disease. *Science*, **302**, 841.
4. Bellucci, A., Navarria, L., Zaltieri, M., Falarti, E., Bodei, S., Sigala, S., Battistin, L., Spillantini, M., Missale, C. and Spano, P. (2011) Induction of the unfolded protein response by α-synuclein in experimental models of Parkinson's disease. *J. Neurochem.*, **116**, 588–605.
5. Cooper, A.A., Gitler, A.D., Cashikar, A., Haynes, C.M., Hill, K.J., Bhullar, B., Liu, K., Xu, K., Strathearn, K.E., Liu, F. *et al.* (2006) Alpha-synuclein blocks ER-Golgi traffic and Rab1 rescues neuron loss in Parkinson's models. *Science*, **313**, 324–328.
6. Kaufman, R.J. (1999) Stress signaling from the lumen of the endoplasmic reticulum: coordination of gene transcriptional and translational controls. *Genes Dev.*, **13**, 1211–1233.
7. Harding, H.P., Calfon, M., Urano, F., Novoa, I. and Ron, D. (2002) Transcriptional and translational control in the Mammalian unfolded protein response. *Annu. Rev. Cell Dev. Biol.*, **18**, 575–599.
8. Holtz, W.A. and O'Malley, K.L. (2003) Parkinsonian mimetics induce aspects of unfolded protein response in death of dopaminergic neurons. *J. Biol. Chem.*, **278**, 19367–19377.
9. Ryu, E.J., Harding, H.P., Angelastro, J.M., Vitolo, O.V., Ron, D. and Greene, L.A. (2002) Endoplasmic reticulum stress and the unfolded protein response in cellular models of Parkinson's disease. *J. Neurosci.*, **22**, 10690–10698.
10. Hoozemans, J.J., van Haastert, E.S., Eikelenboom, P., De Vos, R.A., Rozemuller, J.M. and Scheper, W. (2007) Activation of the unfolded protein response in Parkinson's disease. *Biochem. Biophys. Res. Commun.*, **354**, 707–711.
11. Smith, W.W., Jiang, H., Pei, Z., Tanaka, Y., Morita, H., Sawa, A., Dawson, V.L., Dawson, T.M. and Ross, C.A. (2005) Endoplasmic reticulum stress and mitochondrial cell death pathways mediate A53T mutant alpha-synuclein-induced toxicity. *Hum. Mol. Genet.*, **14**, 3801–3811.
12. Oyadomari, S. and Mori, M. (2004) Roles of CHOP/CHOP in endoplasmic reticulum stress. *Cell Death Differ.*, **11**, 381–389.
13. Silva, R.M., Ries, V., Oo, T.F., Yarygina, O., Jackson-Lewis, V., Ryu, E.J., Lu, P.D., Marciniak, S.J., Ron, D., Przedborski, S. *et al.* (2005) CHOP/GADD153 is a mediator of apoptotic death in substantia nigra dopamine neurons in an in vivo neurotoxin model of parkinsonism. *J. Neurochem.*, **95**, 974–986.
14. Kokame, K., Agarwala, K.L., Kato, H. and Miyata, T. (2000) Herp, a new ubiquitin-like membrane protein induced by endoplasmic reticulum stress. *J. Biol. Chem.*, **275**, 32846–32853.
15. Hori, O., Ichinoda, F., Yamaguchi, A., Tamatani, T., Taniguchi, M., Koyama, Y., Katayama, T., Tohyama, M., Stern, D.M., Ozawa, K. *et al.* (2004) Role of Herp in the endoplasmic reticulum stress response. *Genes Cells*, **9**, 457–469.
16. Chan, S.L., Fu, W., Zhang, P., Cheng, A., Lee, J., Kokame, K. and Mattson, M.P. (2004) Herp stabilizes neuronal Ca2+ homeostasis and mitochondrial function during endoplasmic reticulum stress. *J. Biol. Chem.*, **279**, 28733–28743.
17. Schulze, A., Standera, S., Buerger, E., Kikkert, M., Van Voorden, S., Wiertz, E., Koning, F., Kloetzel, P.M. and Seeger, M. (2005) The ubiquitin-domain protein HERP forms a complex with components of the endoplasmic reticulum associated degradation pathway. *J. Mol. Biol.*, **354**, 1021–1027.
18. Slodzinski, H., Moran, L.B., Michael, G.J., Wang, B., Novoselov, S., Cheetham, M.E., Pearce, R.K. and Graeber, M.B. (2009) Homocysteine-induced endoplasmic reticulum protein (herp) is up-regulated in parkinsonian substantia nigra and present in the core of Lewy bodies. *Clin. Neuropathol.*, **28**, 333–343.
19. Chigurupati, S., Wei, Z., Belal, C., Vandermey, M., Kyriazis, G.A., Arumugam, T.V. and Chan, S.L. (2009) The homocysteine-inducible endoplasmic reticulum stress protein counteracts calcium store depletion and induction of CCAAT enhancer-binding protein homologous protein in a neurotoxin model of Parkinson disease. *J. Biol. Chem.*, **284**, 18323–18333.
20. Chan, S.L., Culmsee, C., Haughey, N., Klapper, W. and Mattson, M.P. (2002) Presenilin-1 mutations sensitize neurons to DNA damage-induced death by a mechanism involving perturbed calcium homeostasis and activation of calpains and caspase-12. *Neurobiol. Dis.*, **11**, 2–19.
21. Chan, S.L., Mayne, M., Holden, C.P., Geiger, J.D. and Mattson, M.P. (2000) Presenilin-1 mutations increase levels of ryanodine receptors and calcium release in PC12 cells and cortical neurons. *J. Biol. Chem.*, **275**, 18195–18200.
22. Kyriazis, G.A., Belal, C., Madan, M., Taylor, D.G., Wang, J., Wei, Z. and Chan, S.L. (2010) Stress-induced switch in Numb isoforms enhances Notch-dependent expression of subtype-specific transient receptor potential channel. *J. Biol. Chem.*, **285**, 6811–6825.
23. Mikoshiba, K. (2007) The IP3 receptor/Ca2+ channel and its cellular function. *Biochem. Soc. Symp.*, **74**, 9–22.

24. Patterson, R.L., Boehning, D. and Snyder, S.H. (2004) Inositol 1, 4, 5-trisphosphate receptors as signal integrators. *Annu. Rev. Biochem.*, **73**, 437–465.
25. Tu, H., Nelson, O., Bezprozvanny, A., Wang, Z., Lee, S.F., Hao, Y.H., Serneels, L., De Strooper, B., Yu, G. and Bezprozvanny, I. (2006) Presenilins form ER Ca2+ leak channels, a function disrupted by familial Alzheimer's disease-linked mutations. *Cell*, **8**, 981–993.
26. Nath, S., Goodwin, J., Engelborghs, Y. and Pountney, D.L. (2011) Raised calcium promotes α-synuclein aggregate formation. *Mol. Cell Neurosci.*, **46**, 516–526.
27. Lee, B., Gai, W. and Laychock, S.G. (2001) Proteasomal activation mediates down-regulation of inositol 1,4,5-trisphosphate receptor and calcium mobilization in rat pancreatic islets. *Endocrinology*, **142**, 1744–1751.
28. Mackrill, J.J. (1998) Possible regulation of the skeletal muscle ryanodine receptor by a polyubiquitin binding subunit of the 26S proteasome. *Biochem. Biophys. Res. Commun.*, **245**, 428–429.
29. Sai, X., Kokame, K., Shiraishi, H., Kawamura, Y., Miyata, T., Yanagisawa, K. and Komano, H. (2003) The ubiquitin-like domain of Herp is involved in Herp degradation, but not necessary for its enhancement of amyloid beta-protein generation. *FEBS Lett.*, **553**, 151–156.
30. Giasson, B.I., Duda, J.E., Quinn, S.M., Zhang, B., Trojanowski, J.Q. and Lee, V.M. (2002) Neuronal alpha-synucleinopathy with severe movement disorder in mice expressing A53T human alpha-synuclein. *Neuron*, **34**, 521–533.
31. Hajnoczky, G., Csordas, G., Madesh, M. and Pacher, P. (2000) Control of apoptosis by IP(3) and ryanodine receptor driven calcium signals. *Cell Calcium*, **28**, 349–363.
32. Mattson, M.P. (2007) Calcium and neurodegeneration. *Aging Cell*, **6**, 337–350.
33. Frandsen, A. and Schousboe, A. (1991) Dantrolene prevents glutamate cytotoxicity and Ca2+ release from intracellular stores in cultured cerebral cortical neurons. *J. Neurochem.*, **56**, 1075–1078.
34. Guo, Q., Sopher, B.L., Furukawa, K., Pham, D.G., Robinson, N., Martin, G.M. and Mattson, M.P. (1997) Alzheimer's presenilin mutation sensitizes neural cells to apoptosis induced by trophic factor withdrawal and amyloid beta-peptide: involvement of calcium and oxyradicals. *J. Neurosci.*, **17**, 4212–4222.
35. Higo, T., Hamada, K., Hisatsune, C., Nukina, N., Hashikawa, T., Hattori, M., Nakamura, T. and Mikoshiba, K. (2010) Mechanism of ER stress-induced brain damage by IP(3) receptor. *Neuron*, **68**, 865–878.
36. Kim, T.Y., Kim, E., Yoon, S.K. and Yoon, J.B. (2008) Herp enhances ER-associated protein degradation by recruiting ubiquilins. *Biochem. Biophys. Res. Commun.*, **369**, 741–746.
37. Miura, H., Hashida, K., Sudo, H., Awa, Y., Takarada-Iemata, M., Kokame, K., Takahashi, T., Matsumoto, M., Kitao, Y. and Hori, O. (2010) Deletion of Herp facilitates degradation of cytosolic proteins. *Genes Cells*, **15**, 843–853.
38. Madesh, M., Hawkins, B.J., Milovanova, T., Bhanumathy, C.D., Joseph, S.K., Ramachandrarao, S.P., Sharma, K., Kurosaki, T. and Fisher, A.B. (2005) Selective role for superoxide in InsP3 receptor-mediated mitochondrial dysfunction and endothelial apoptosis. *J. Cell Biol.*, **170**, 1079–1090.
39. Deniaud, A., Sharaf el dein, O., Maillier, E., Poncet, D., Kroemer, G., Lemaire, C. and Brenner, C. (2008) Endoplasmic reticulum stress induces calcium-dependent permeability transition, mitochondrial outer membrane permeabilization and apoptosis. *Oncogene*, **27**, 285–299.
40. Jiang, P., Gan, M., Ebrahim, A.S., Lin, W.L., Melrose, H.L. and Yen, S.H. (2010) ER stress response plays an important role in aggregation of α-synuclein. *Mol. Neurodegener.*, **5**, 56.
41. Mouatt-Prigent, A., Agid, Y. and Hirsch, E.C. (1994) Does the calcium binding protein calretinin protect dopaminergic neurons against degeneration in Parkinson's disease? *Brain Res.*, **668**, 62–70.
42. Von Lewinski, F., Fuchs, J., Vanselow, B.K. and Keller, B.U. (2008) Low Ca2+ buffering in hypoglossal motoneurons of mutant SOD1 (G93A) mice. *Neurosci. Lett.*, **445**, 224–228.
43. Kikuchi, H., Almer, G., Yamashita, S., Guégan, C., Nagai, M., Xu, Z., Sosunov, A.A., McKhann, G.M. 2nd and Przedborski, S. (2006) Spinal cord endoplasmic reticulum stress associated with a microsomal accumulation of mutant superoxide dismutase-1 in an ALS model. *Proc. Natl Acad. Sci. USA*, **103**, 6025–6030.